BCL3 rearrangements in B-cell lymphoid neoplasms occur in two breakpoint clusters associated with different diseases

Anna Carbó-Meix,[1*] Francesca Guijarro,[1,2*] Luojun Wang,[2*] Marta Grau,[1*] Romina Royo,[3] Gerard Frigola,[1,2] Heribert Playa-Albinyana,[1,4] Marco M. Bühler,[5] Guillem Clot,[1] Martí Duran-Ferrer,[1,4] Junyan Lu,[6] Isabel Granada,[7] Maria-Joao Baptista,[7] José-Tomás Navarro,[7] Blanca Espinet,[8] Anna Puiggros,[8] Gustavo Tapia,[9] Laura Bandiera,[10] Gabriella De Canal,[10] Emanuela Bonoldi,[10] Fina Climent,[11] Inmaculada Ribera-Cortada,[12] Mariana Fernández-Caballero,[7] Esmeralda de la Banda,[13] Janilson do Nascimento,[14] Alberto Pineda,[15] Dolors Vela,[16] María Rozman,[2] Marta Aymerich,[1,2] Charlotte Syrykh,[17] Pierre Brousset,[17,18,19] Miguel Perera,[20] Lucrecia Yáñez,[21] Jesús Xavier Ortin,[22] Esperanza Tuset,[23] Thorsten Zenz,[24] James R. Cook,[25] Steven H. Swerdlow,[26] José I. Martín-Subero,[1,4,27,28] Dolors Colomer,[1,2,4,27] Estella Matutes,[2] Sílvia Beà,[1,2,4,27] Dolors Costa,[1,2,4] Ferran Nadeu[1,4#] and Elías Campo[1,2,4,27#]

[1]Institut d'Investigacions Biomèdiques August Pi i Sunyer (IDIBAPS), Barcelona, Spain; [2]Hematopathology Section, Pathology Laboratory, Hospital Clínic de Barcelona, Barcelona, Spain; [3]Barcelona Supercomputing Center (BSC), Barcelona, Spain; [4]Centro de Investigación Biomédica en Red de Cáncer (CIBERONC), Madrid, Spain; [5]Department of Pathology and Molecular Pathology, University Hospital Zürich, Zürich, Switzerland; [6]European Molecular Biology Laboratory, Heidelberg, Germany; [7]Department of Hematology, Institut Català d'Oncologia, Hospital Germans Trias i Pujol, Josep Carreras Research Institute, Universitat Autònoma de Barcelona, Badalona, Spain; [8]Molecular Cytogenetics Laboratory, Department of Pathology, Hospital del Mar, Barcelona, Spain and Translational Research on Hematological Neoplasms Group (GRETNHE) - Institut Hospital del Mar d'Investigacions Mèdiques (IMIM), Barcelona, Spain; [9]Department of Pathology, Hospital Germans Trias i Pujol, Badalona, Spain; [10]Dipartimento Ematologia, Oncologia e Medicina Molecolare, Anatomia Istologia Patologica e Citogenetica, Niguarda Cancer Center, Milano, Italy; [11]Department of Pathology, Hospital Universitari de Bellvitge, Institut d'Investigació Biomèdica de Bellvitge (IDIBELL), L'Hospitalet De Llobregat, Spain; [12]Department of Pathology, Hospital Nostra Senyora de Meritxell, Escaldes-Engordany, Principat d'Andorra; [13]Hematology Laboratory, Hospital Universitari Bellvitge, Institut d'Investigació Biomèdica de Bellvitge (IDIBELL), L'Hospitalet De Llobregat, Spain; [14]Department of Hematology, Hospital Joan XXIII, Institut Català d'Oncologia, Tarragona, Spain; [15]Department of Hematology, Fundació Hospital de l'Esperit Sant, Badalona, Spain; [16]Hematologia Clínica, Hospital General de Granollers, Granollers, Spain; [17]Department of Pathology, Toulouse University Hospital Center, Cancer Institute University of Toulouse-Oncopole, Toulouse, France; [18]INSERM UMR1037 Cancer Research Center of Toulouse (CRCT), ERL 5294 National Center for Scientific Research (CNRS), University of Toulouse III Paul-Sabatier, Toulouse, France; [19]Institut Carnot Lymphome CALYM, Laboratoire d'Excellence 'TOUCAN', Toulouse, France; [20]Hematology Department, Hospital Dr Negrín, Las Palmas de Gran Canaria, Spain; [21]Hematology Department, Hospital Universitario Marqués de Valdecilla-Instituto de Investigación Valdecilla (IDIVAL), Santander, Spain; [22]Hematology Department, Hospital Verge de la Cinta, Tortosa, Spain; [23]Hematology Department, Institut Català d'Oncologia, Hospital Dr. Josep Trueta, Institut d'Investigació Biomèdica de Girona (IDIBGI), Girona, Spain; [24]Department of Medical Oncology and Hematology, University Hospital and University of Zürich, Zurich, Switzerland; [25]Pathology and Laboratory Medicine Institute, Cleveland Clinic, Cleveland, OH, USA; [26]Department of Pathology, University of Pittsburgh School of Medicine, Pittsburgh, PA, USA; [27]Department of Fonaments Clinics, Universitat de Barcelona, Barcelona, Spain and [28]Institució Catalana de Recerca i Estudis Avançats (ICREA), Barcelona, Spain

AC-M, FG, LW and MG contributed equally as first authors.
#FN and EC contributed equally as senior authors.

Correspondence: E. Campo
ecampo@clinic.cat

Received: March 23, 2022
Accepted: July 31, 2023.
Early view: August 10, 2023.

https://doi.org/10.3324/haematol.2023.283209

Abstract

The t(14;19)(q32;q13) often juxtaposes *BCL3* with immunoglobulin heavy chain (IGH) resulting in overexpression of the gene. In contrast to other oncogenic translocations, *BCL3* rearrangement (*BCL3*-R) has been associated with a broad spectrum of lymphoid neoplasms. Here we report an integrative whole-genome sequence, transcriptomic, and DNA methylation analysis of 13 lymphoid neoplasms with *BCL3-R*. The resolution of the breakpoints at single base-pair revealed that they occur in two clusters at 5' (n=9) and 3' (n=4) regions of *BCL3* associated with two different biological and clinical entities. Both breakpoints were mediated by aberrant class switch recombination of the IGH locus. However, the 5' breakpoints (upstream) juxtaposed *BCL3* next to an IGH enhancer leading to overexpression of the gene whereas the 3' breakpoints (downstream) positioned *BCL3* outside the influence of the IGH and were not associated with its expression. Upstream *BCL3*-R tumors had unmutated IGHV, trisomy 12, and mutated genes frequently seen in chronic lymphocytic leukemia (CLL) but had an atypical CLL morphology, immunophenotype, DNA methylome, and expression profile that differ from conventional CLL. In contrast, downstream *BCL3*-R neoplasms were atypical splenic or nodal marginal zone lymphomas (MZL) with mutated IGHV, complex karyotypes and mutated genes typical of MZL. Two of the latter four tumors transformed to a large B-cell lymphoma. We designed a novel fluorescence *in situ* hybridization assay that recognizes the two different breakpoints and validated these findings in 17 independent tumors. Overall, upstream or downstream breakpoints of *BCL3*-R are mainly associated with two subtypes of lymphoid neoplasms with different (epi)genomic, expression, and clinicopathological features resembling atypical CLL and MZL, respectively.

Introduction

The t(14;19)(q32;q13) is a balanced translocation found in less than 1% of lymphoid neoplasms that often leads to the juxtaposition of *BCL3* (B-cell leukemia/lymphoma 3) with regulatory elements of the immunoglobulin heavy chain (IGH) gene, resulting in the overexpression of the gene.[1] *BCL3* encodes an IκB-like nuclear protein that regulates NF-κB activity apparently as a molecular adaptor between NF-κB transcription factors and nuclear co-activator and co-repressor complexes.[2] Although the function of BCL3 in B cells is not fully understood, this gene seems to be involved in regulation of cell proliferation, differentiation, and survival.[3,4] In transgenic mice, Bcl3 overexpression promoted accumulation of mature B cells but it was not sufficient to drive malignant transformation.[5]

Chromosomal translocations activating oncogenes in lymphoid neoplasms are usually associated with relatively specific tumor subtypes. However, the t(14;19) and *BCL3* rearrangement (*BCL3*-R) have been identified in a broad spectrum of different tumor subtypes.[6,7] Most patients have been diagnosed with chronic lymphocytic leukemia (CLL), atypical CLL, or transformed CLL. These tumors frequently have an unmutated IGHV (U-IGHV) and trisomy 12. However, they also have atypical features for CLL, including cytology and immunophenotype not characteristic of CLL, frequent IGHV stereotype #8, and aggressive behavior in some series.[6-9] Some authors have suggested that B-cell neoplasms carrying the t(14;19) could represent an entity different from CLL.[6] In addition to these tumors resembling CLL, the t(14;19) and *BCL3*-R have been also identified in diffuse large B-cell lymphomas (DLBCL), marginal zone lymphomas (MZL), splenic small B-cell lymphomas, and tumors diagnosed as B-cell non-Hodgkin lymphomas, some of them with evidence of transformation.[6,7] Whether this diversity of entities associated with *BCL3*-R corresponds to a real biological promiscuity is not clear. Some reports included tumors with the t(14;19) by cytogenetics without the specific analysis of *BCL3*-R. Since this translocation may rearrange genes other than *BCL3*, it is possible that some of the series reported may have included tumors that did not involve *BCL3*. Furthermore, some studies included tumors for which the pathological features were not thoroughly reviewed.[6,7]

The purposes of this study were to characterize the genomic configuration of *BCL3*-R in B-cell neoplasms and to understand the clinical and biological significance of this alteration using an integrative (epi)genomic and transcriptomic analysis in a cohort of patients with available clinical and pathological characteristics.

Methods

Patients and samples

We searched the cytogenetic files of lymphoid B-cell neoplasms with t(14;19) or *BCL3*-R in three institutions from 2008 to 2019. Fluorescence *in situ* hybridization (FISH) with dual-color break-apart probes for IGH and *BCL3* genes (XL IGH BA and XL *BCL3* BA, Metasystems) was performed in patients with available material. Patients with t(14;19), but lacking confirmation of *BCL3*-R, were excluded. Overall, 13 B-cell neoplasms carrying *BCL3*-R, with available material for genomic studies, were identified (Table 1; *Online Supplementary Figure S1*; *Online Supplementary Table S1*). These cases represent 0.28% of all small B-cell lymphomas

studied genetically. The initial diagnoses were atypical CLL (aCLL) (n=5), SLL/CLL (n=3), splenic marginal zone lymphoma (SMZL) (n=3), lymphoplasmacytic lymphoma (n=1), and unclassifiable low-grade B-cell leukemic neoplasm (n=1). Tumor DNA was obtained from cryopreserved blood cells or frozen tumor tissue in all patients, germline DNA from non-neoplastic blood cells or saliva (n=10), and RNA from peripheral blood purified cells (n=5) or frozen tissue (n=2). Informed consent was obtained from all patients, and the study was approved by the Ethics Committee of the Hospital Clínic of Barcelona.

Genomic studies

Whole-genome sequencing (WGS) of the 13 tumors and 10 paired normal DNA samples was performed using the TruSeq DNA PCR Free or TruSeq DNA nano library preparation. Raw reads were mapped to the human reference genome (GRCh37) using the BWA-MEM algorithm.[10] Immunoglobulin gene rearrangements were extracted using IgCaller (version 1.1)[11] and annotated using IMGT/V-QUEST.[12] Genomic alterations were identified using a multi-caller bioinformatics approach (*Online Supplementary Appendix*).[13] Driver mutations were studied considering a list of 247 recurrently mutated genes in B-cell neoplasms (*Online Supplementary Appendix*; *Online Supplementary Table S2*). Total RNA sequencing (RNA-seq) was performed in seven tumors with *BCL3*-R and nine CLL without *BCL3*-R. Raw data were analyzed as previously described (*Online Supplementary Appendix*)[13] using the DESeq2 package.[14] mRNA-seq data from our International Cancer Genome Consortium CLL cohort were used for comparison.[15] DNA methylation profiles of ten *BCL3*-R tumors were generated using EPIC methylation arrays. Similar data from 85 CLL were obtained for comparison from two previous publications: cohort 1 (C1) included 12 CLL from our institution,[13] and cohort 2 (C2) 73 CLL from University Hospital Heidelberg.[16] Data analyses were performed using minfi and limma packages.[17,18] The AME tool from the MEME suite[19] was used for enrichment analysis of known motifs (2022 JASPAR database; *Online Supplementary Appendix*).[20] WGS, RNA-seq, and DNA methylation data are deposited in the European Genome-phenome Archive.

Immunohistochemistry

BCL3 protein expression was studied by immunohistochemistry (IHC) in tumors with formalin-fixed paraffin-embedded tissue. Tissue sections (3 μm) were stained using a Leica Bond-MAX stainer (Leica Biosystems) and the anti-BCL3 primary antibody (23959-1-AP; Proteintech) (*Online Supplementary Appendix*).

Custom *BCL3* fluorescence *in situ* hybridization

Custom *BCL3* break-apart FISH probes to detect 5' and 3' *BCL3* breakpoints were designed using three differentially labeled BAC clones: RP11-927F16 (spectrum orange), CTD-2608C5 (spectrum aqua), and RP11-423N20 (spectrum green) from the Children´s Hospital Oakland Research Institute library obtained from the Molecular Cytogenetics Platform of IMIM (Barcelona, Spain) and Life Technologies. BAC extraction and labeling, slide preparation, and hybridization were performed according to standard procedures.[21]

Results

Genomic characterization of the *BCL3* rearrangement

We first characterized the breakpoints of the *BCL3* rearrangement at base-pair resolution using WGS data from 13 tumors (*Online Supplementary Table S3*). *BCL3* was rearranged with the IGH region as a clonal event in all but one tumor (3646), in which the number of reads suggested a subclonal distribution. All tumors had breakpoints on chromosome 14 within class switch recombination (CSR) regions of the IGH locus (Figure 1A). Breakpoints occurred in IGHA2 (n=1), IGHG2 (n=3), IGHA1 (n=4), IGHG1 (n=3), and IGHG3 (n=3). Breakpoints on chromosome 19 (chr19) were found upstream of the 5' untranslated region (UTR) of *BCL3* in eight of 13 (61.5%) tumors (Figure 1A). These breakpoints occurred within a window of 13 kb, and the translocation juxtaposed *BCL3* downstream of the CSR (Figure 1B). Notably, all eight tumors had U-IGHV, six had 100%, and two had 99.6% IGHV identity with the germline (Figure 1A; *Online Supplementary Table S4*). One additional tumor (3698) with mutated IGHV (M-IGHV) (94.4% identity) had a breakpoint further upstream of *BCL3* truncating *CEACAM16*, although the result of the translocation also placed *BCL3* downstream of the CSR (Figures 1A, C). The four remaining tumors had breakpoints downstream of *BCL3*, two within *CBLC*, one in *BCAM*, and one after *NECTIN2* (Figure 1A). In these four translocations, *BCL3* was not located after the CSR of IGH; therefore, it does not seem to be the target of the translocation (Figure 1C). All tumors carrying the breakpoint downstream of *BCL3* had M-IGHV with <98% germline identity.

In order to determine the influence of the chr19 breakpoint on *BCL3* expression, we studied 12 tumors, seven by RNA-seq (6 with the breakpoint upstream and 1 downstream) and seven by IHC (3 upstream and 4 downstream). Two tumors were studied using both approaches (*Online Supplementary Table S5*). Eight tumors carrying the upstream *BCL3*-R, including one further upstream (3698), overexpressed *BCL3* in comparison to CLL without this rearrangement (Figures 2A, B). No protein expression was detected by IHC in ten additional nodal CLL with unmutated IGHV (U-CLL) with trisomy 12 and without *BCL3*-R. In contrast, the four tumors downstream *BCL3*-R did not express *BCL3* (Figures 2A, B). The only downstream *BCL3*-R tumor with RNA available (3676) showed overexpression

Table 1. Clinical and pathological features of 13 patients with *BCL3* rearrangement.

	Total N=13	Upstream *BCL3*-R N=9	Downstream *BCL3*-R N=4	*P*
Clinical data at diagnosis				
Median age in years (range)	69 (50-81)	69 (50-78)	64 (53-81)	1
Male, N (%)	7 (54)	5 (56)	2 (50)	1
ALC, x10^9/L (range)	8.1 (0.9-161.8)	9 (2.9-161.8)	1 (0.9-2.9)	0.01
Lymphadenopathy, N (%)	3 (25)	3 (38)	0	0.49
Splenomegaly, N (%)	4 (33)	1 (13)	3 (75)	0.07
B symptoms, N (%)	3 (25)	1 (13)	2 (50)	0.24
Clinical data at follow-up				
Need for treatment, N (%)	9 (69)	5 (56)	4 (100)	0.23
Median time in years to first treatment	2.6	4.6	0.9	0.7
Large B-cell lymphoma transformation, N (%)	2 (15)	0	2 (50)	0.08
Median survival time in years	10.5	11.1	10.5	0.5
Genetics, N (%)				
Trisomy 12	7 (54)	7 (78)	0	0.04
Complex karyotype	8 (61)	6 (67)	2 (67)	1
Unmutated *IGHV* status	8 (61)	8 (89)	0	0.007
Deletion 11q	2 (15)	1 (11)	1 (25)	1
TP53 mutation	0	0	0	
Deletion 17p	0	0	0	
Phenotype				
Flow cytometry, N (%)				
Typical for CLL*	3 (23)	3 (33)	0	
Bright sIg	8 (61)	4 (44)	4 (100)	
Bright B-cell markers	9 (69)	5 (56)	4 (100)	
CD5$^+$	9 (69)	9 (100)	0	
CD43$^+$	7 (58)	6 (67)	1 (33)	
CD23$^+$	6 (50)	6 (67)	0	
CD200$^+$	9 (75)	8 (89)	1 (33)	
Immunohistochemistry, N/N				
CD5$^+$	3/7	3/4	0/3	
CD23$^+$	4/7	2/4 strong, 2/4 weak	0/3	
LEF1$^+$	0/7	0/4	0/3	
BCL3$^+$	3/6	3/3	0/3	

Quantitative parameters are expressed as median (range). *Typical chronic lymphocytic leukemia (CLL) immunophenotype CD19$^+$ with dim expression of CD20, CD22, CD79b, CD5$^+$, CD23$^+$, CD43$^+$, CD200$^+$, and FMC7$^-$. *BCL3*-R: *BCL3* rearrangement; IGHV: variable region of the immunoglobulin heavy chain gene; ALC: absolute lymphocyte count; sIg: surface immunoglobulins.

of *NECTIN2*, which was negative in all upstream *BCL3*-R tumors (Figures 2A).

Overall, the location of the chr19 breakpoint distinguishes two main subgroups: i) tumors with upstream *BCL3*-R breakpoints, which overexpress *BCL3* and are enriched in U-IGHV, and ii) tumors with downstream *BCL3*-R breakpoints, which do not overexpress *BCL3* and carry M-IGHV.

Genomic landscape

Tumors with upstream *BCL3*-R, excluding the three patients lacking normal DNA, had significantly fewer somatic mutations (mean 2,511; range, 1,825-3,165; n=7) than tumors with downstream *BCL3*-R (mean 6,271.7; range, 4,535-9,125; n=3) (*P*<0.05; Figure 3A, B; *Online Supplementary Table S6*). Mutational signature analysis identified the presence of SBS1, SBS5, and SBS8 in all cases, SBS18 in seven cases, and SBS9 in three tumors with M-IGHV (*Online Supplementary Figure S2*; *Online Supplementary Table S7*). In addition, we searched for activation-induced deaminase (AID) motifs in the mutations occurring in IGH locus between the constant gene and class switch regions. We found that 17 of 25 (68%) mutations occurred in AID motifs (*Online Supplementary Table S8*).

The driver mutations in the upstream *BCL3*-R subgroup were very heterogeneous, with only *MED12* and *FAT4* recurrently mutated in two tumors each. Other mutated genes have also been frequently described in CLL (*ATM*, *NOTCH1*, *POT1*, *KHL6*). In the four downstream *BCL3*-R tumors, two carried mutations in *KMT2D*, *NOTCH2*, and *KLF2*, frequently seen in MZL, whereas the remaining two tu-

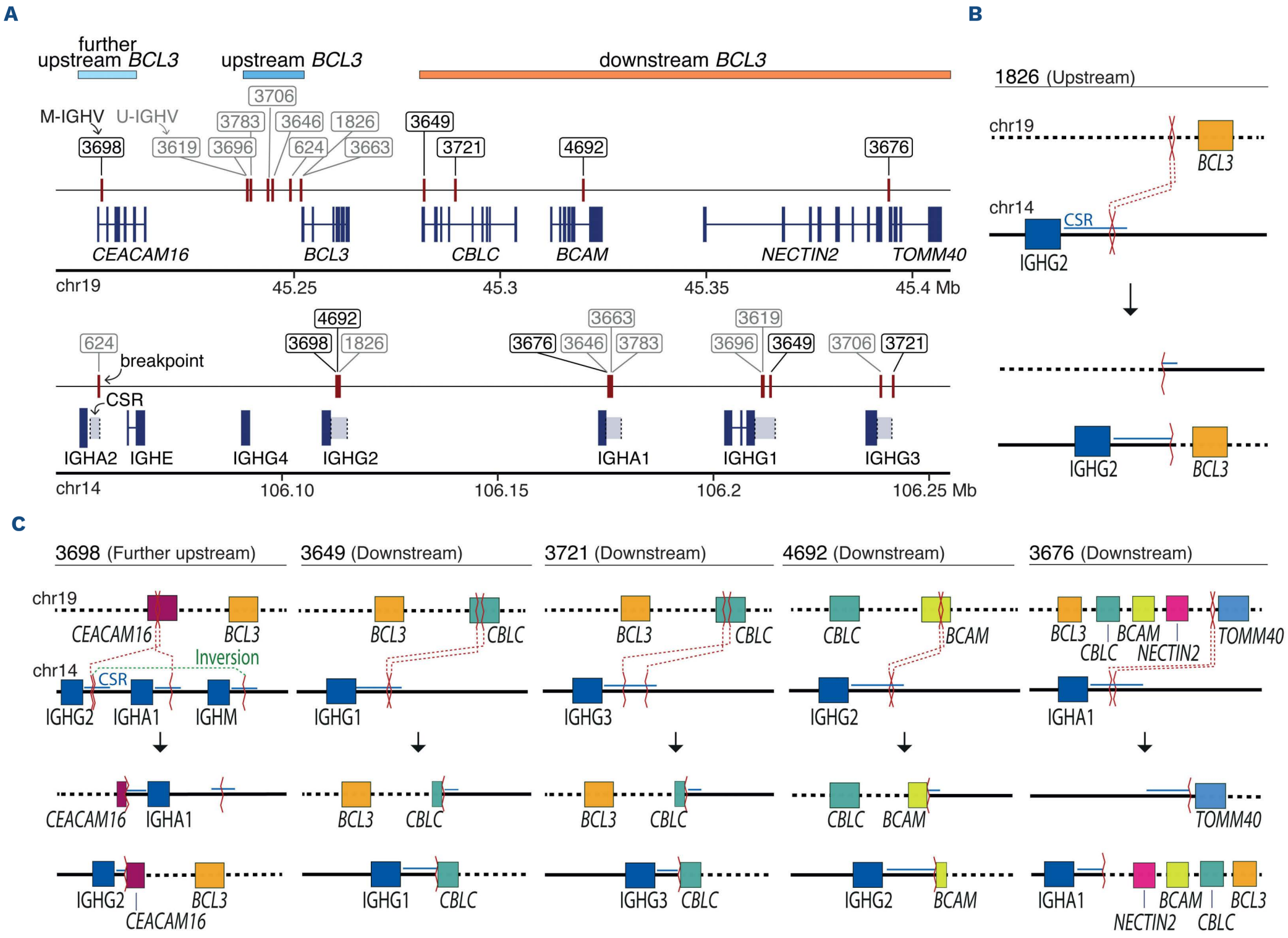

Figure 1. Characterization of the breakpoints derived from the t(14;19) at base-pair resolution. (A) Representation of the breakpoints on chromosome 19 (chr19) and chr14 for each patient (red vertical line). Unmutated variable region of the immunoglobulin heavy chain gene (U-IGHV) and mutated IGHV (M-IGHV) tumors are represented in gray and black labels, respectively. Tumors are classified based on the breakpoint on chromosome 19 (chr19): further upstream *BCL3* (pale blue), upstream *BCL3* (blue), and downstream *BCL3* (orange). (B) Schema of the most recurrent translocation pattern observed in the upstream *BCL3* subgroup with IGH and its corresponding class switch recombination (CSR) located upstream *BCL3*, suggesting a constitutive upregulation of *BCL3*. (C) Depiction of 5 patients, 1 with the translocation further upstream *BCL3* and 4 with the translocation downstream *BCL3*. In the further upstream tumor (3698), the t(14;19) truncates *CEACAM16* and, similar to upstream *BCL3* translocations, IGH is located 5' of *BCL3* suggesting a constitutive upregulation of this gene. In the downstream tumors, the t(14;19) affects 3 different genes (*CBLC*, *BCAM*, *NECTIN2*) located downstream of *BCL3*. The resulting derivatives of the t(14;19) suggest that *BCL3* is not placed under the regulation of the enhancers of the IGH and, therefore, its expression remains unchanged.

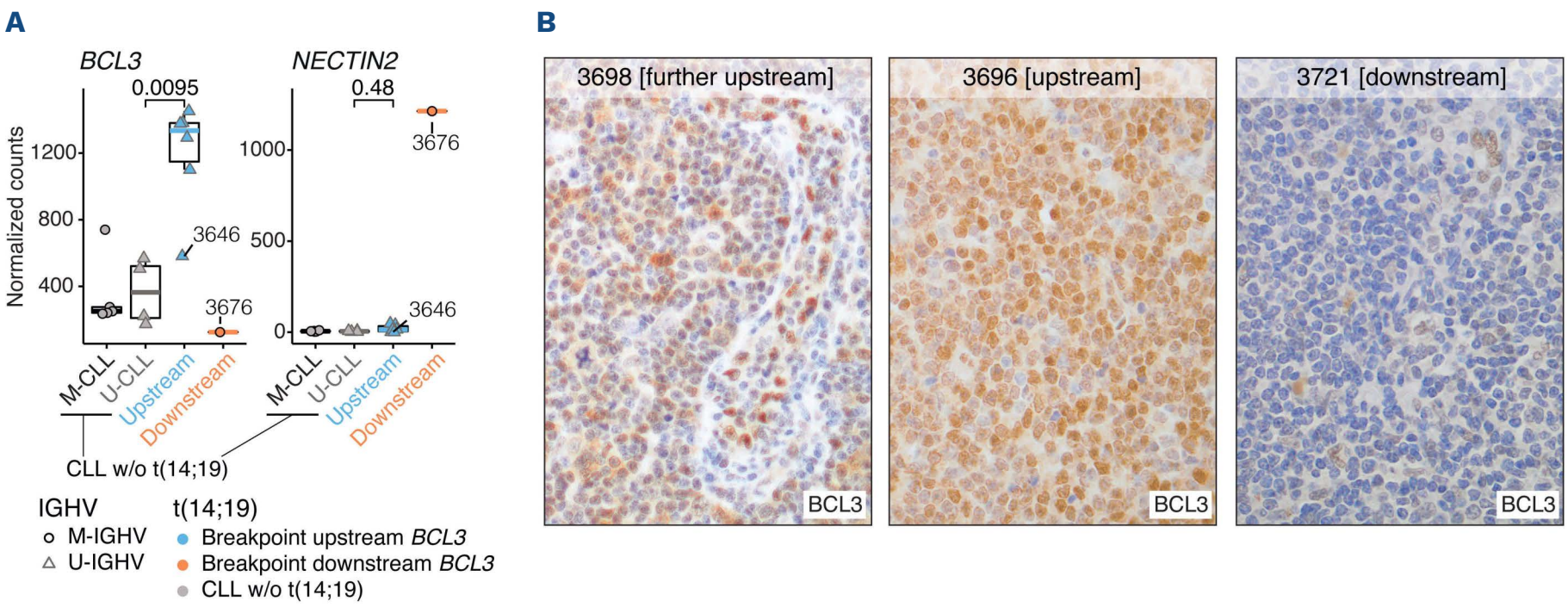

Figure 2. BCL3 expression in upstream and downstream tumors with *BCL3* rearrangement. (A) RNA-sequencing data shows that BCL3 is upregulated in the upstream *BCL3* tumors, except tumor 3646 carrying a subclonal t(14;19), compared to unmutated chronic lymphocyitc leukemia (U-CLL). Contrarily, the downstream *BCL3* tumor (3676) upregulated NECTIN2 while showed lower BCL3 expression than any of the upstream and CLL tumors. (B) Immunohistochemistry images (400x) displaying a positive BCL3 expression in the further upstream tumor and in a representative upstream tumor, but not in a representative downstream tumor.

mors had recurrent mutations in *TBL1XR1*, detected in aggressive lymphomas, but also in some MZL (Figure 3A).

In terms of CNA, upstream *BCL3*-R tumors had a significantly lower genomic complexity (mean 2.9; range, 1-9; n=9) than downstream *BCL3*-R tumors (mean 11.7; range, 5-19; n=3) (P<0.05; Figure 3B; *Online Supplementary Table S9*). All but one upstream *BCL3*-R tumor carried trisomy 12, but this aberration was not observed in any of the downstream *BCL3*-R tumors (Figures 3B, C; *Online Supplementary Figure S3*). In line with the copy number alterations (CNA), the number of structural variations (SV) was lower in upstream *BCL3*-R tumors than in downstream *BCL3*-R tumors (mean 4.8 SV; range, 2-10 [n=6] *vs.* 18 SV; range, 8-28 [n=3], respectively) (Figures 3B; *Online Supplementary Figure S4*; *Online Supplementary Table S10*).

Gene expression profiling

In order to determine the gene expression profile of the *BCL3*-R tumors, we compared the RNA-seq data of seven *BCL3*-R tumors (6 with upstream and 1 downstream breakpoint) with nine CLL (4 U-CLL and 5 mutated IGHV [M-CLL]). An unsupervised principal component analysis (PCA) suggested that upstream *BCL3*-R tumors displayed a distinct gene expression profile with some similarities with both M-CLL and U-CLL, whereas the downstream *BCL3*-R tumor did not cluster with any of the other tumors (Figure 4A). Then, we conducted a differential expression analysis (DEA) between upstream *BCL3*-R tumors, all U-IGHV with trisomy 12, four CLL with U-IGHV, and one with trisomy 12 (excluding tumor 3646 with subclonal *BCL3*-R). This analysis identified 1,298 differentially expressed genes (DEG): 578 upregulated and 720 downregulated in the upstream *BCL3*-R subgroup (q<0.05; Figure 4B; *Online Supplementary Table S11*). These genes showed similar expression levels in U- and M-CLL (Figure 4B; *Online Supplementary Table S12*). Significant expression differences were found in genes previously described as characteristically down- or upregulated in CLL compared with other B-cell neoplasms.[22-24] Among them, upstream *BCL3*-R tumors had significant overexpression of *EBF1*, usually not expressed in CLL, and, in contrast, downregulation of *LEF1*, *FMOD*, *ADTRP*, *CLNK*, *IGSF3*, and *TCF4*, frequently overexpressed in CLL (Figure 4C).

To rule out a potential confounding effect of trisomy 12, we performed a DEA between 16 U-CLL with trisomy 12 and 49 U-CLL without trisomy 12 using data from our ICGC CLL cohort.[15] These analyses identified 1,527 DEG (q<0.05, absolute (log2 fold change [FC])>0.1; *Online Supplementary Table S13*). Among them, only 129 (9.9%) were shared by the upstream *BCL3*-R tumors, suggesting that most DEG observed in *BCL3*-R tumors were not related to trisomy 12 (Figure 4D). Interestingly, most CLL-specific genes modulated in the upstream *BCL3*-R tumors appeared to be independent of trisomy 12 in U-CLL (Figure 4D; *Online Supplementary Figure S5A*).

Gene set enrichment analyses of upstream *BCL3*-R tumors and U-CLL with trisomy 12 showed that, while both subgroups of tumors shared some genes related to trisomy 12, most other pathways identified were expressed at lower levels in *BCL3*-R tumors, such as B-cell receptor (BCR) signaling or TNFα signaling via NF-κB (*Online Supplementary Figure S5B*; *Online Supplementary Tables S14,*

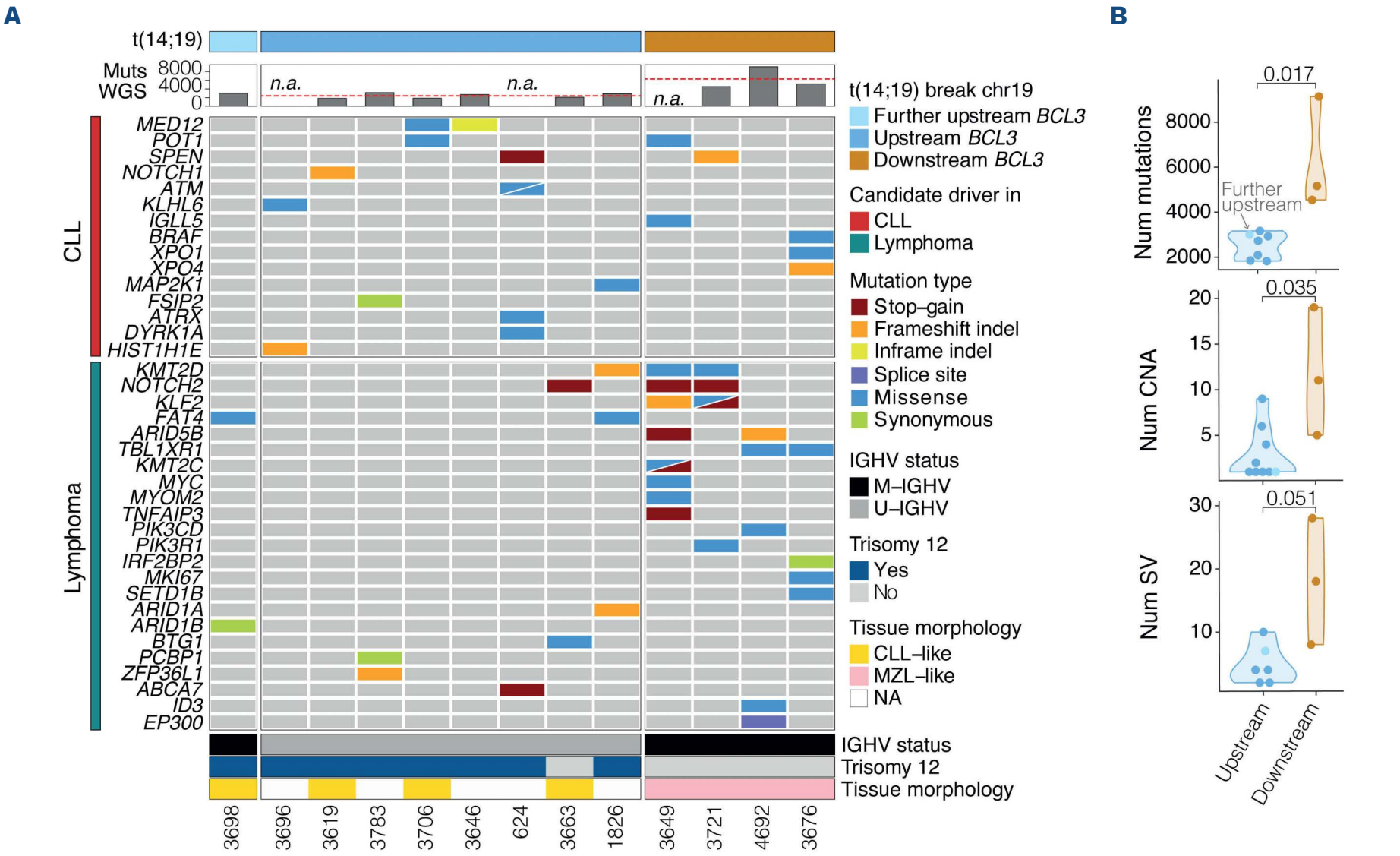

Figure 3. Mutations and structural alterations in B-cell neoplasms with t(14;19) and *BCL3* rearrangement identified by whole-exome sequencing. (A) Oncoprint representation of driver gene mutations frequently observed in chronic lymphocytic leukemia (CLL) (red) or in other B-cell lymphomas (blue-green). Total number of mutations are not reported in samples 3649, 3696, and 624 due to the lack of germline DNA (*Online Supplementary Appendix*; *Online Supplementary Table S1*). (B) Comparison of the number of mutations, copy number alterations (CNA) and structural variations (SV) between upstream *BCL3* rearrangement (*BCL3*-R) and downstream *BCL3*-R tumors. (C) Copy number profile of *BCL3*-R tumors. Tumors are shown in rows and chromosomes in columns. The variable region of the immunoglobulin heavy chain gene (IGHV) mutational status, breakpoint location on chromosome 19, and number of CNA are shown on the right. Sample 3649 had an estimated tumor cell content of 20% that allowed the detection of driver somatic mutations and the *BCL3*-R but was not sufficient for a proper analysis of CNA (*Online Supplementary Appendix*; *Online Supplementary Table S1*). MZL: marginal zone lymphoma; CNN-LOH: copy number neutral loss of heterozygosity; Num: number; mut: mutational; NA: not available; M-IGHV: mutated IGHV; U-IGHV: unmutated IGHV.

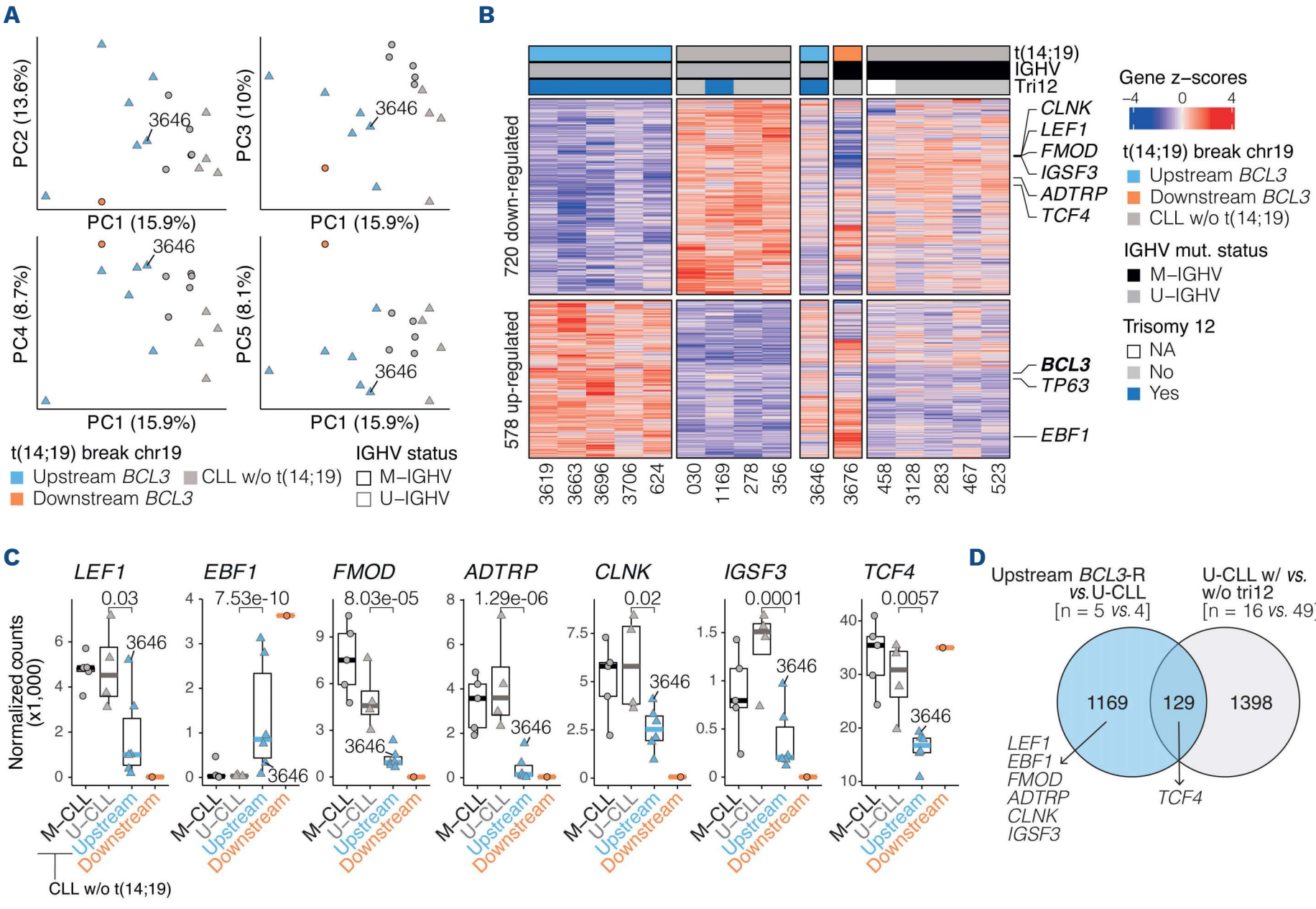

Figure 4. Gene expression profile of upstream tumors with *BCL3* rearrangement. (A) Principal component analysis of RNA sequencing data of 6 upstream *BCL3* rearrangement (*BCL3*-R) tumors, 1 downstream *BCL3*-R tumor, and 9 chronic lymphocytic leukemia (CLL) (1st component is shown against 2nd, 3rd, 4th and 5th components). (B) Heatmap of the differential gene expression analysis between 5 upstream *BCL3*-R tumors and 4 unmutated CLL (U-CLL), also compared to 1 tumor with downstream *BCL3*-R tumor and CLL without t(14;19). Tumor 3646 was excluded from the analysis due to its subclonal *BCL3*-R. Hallmark CLL genes differentially expressed between *BCL3*-R tumors and CLL are flagged. (C) Expression of CLL hallmark genes in the upstream *BCL3*-R tumors compared to U-CLL. Q-values are from the differential gene expression analysis. (D) Venn diagram showing the overlap of the differentially expressed genes among upstream *BCL3*-R *versus* U-CLL and U-CLL with *versus* without trisomy 12. Hallmark CLL genes are highlighted. IGHV: variable region of the immunoglobulin heavy chain gene; M-IGHV: mutated IGHV; U-IGHV: unmutated IGHV; NA: not available; M-CLL: mutated CLL; w/o: without.

S15). The lower BCR-signaling capacity of *BCL3*-R tumors was confirmed by measuring Ca^{2+} mobilization upon BCR stimulation with IgM (*Online Supplementary Figure S6*; *Online Supplementary Appendix*). These findings suggest that, although upstream *BCL3*-R tumors share a subset of commonly expressed genes in CLL carrying trisomy 12, they also have a remarkably distinct profile.

DNA methylation

We analyzed the DNA methylation profile of eight upstream *BCL3*-R tumors, one of which was subclonal, and two downstream *BCL3*-R, and compared them with that of 85 CLL classified as naive-like CLL (n-CLL) (n=33), intermediate CLL (i-CLL) (n=7), or memory-like (m-CLL) (n=45),[25,26] and seven normal B-cell subsets (2 naive, 1 germinal center, 3 memory, and 1 plasma cell). We first performed PCA using 764159 CpG (Figure 5A). Principal component 1 (PC1) reflected the variability related to the proliferative history of the cells captured by the epiCMIT score,[26] whereas PC2 grouped samples based on the cell of origin, in which upstream *BCL3*-R clustered with n-CLL (Figure 5A). Upstream *BCL3*-R tumors had a higher proliferative history than n-CLL. This observation was confirmed by comparing epiCMIT scores between *BCL3*-R and n-CLL in the C1 (P=0.0043) and C2 (P=0.00016) CLL cohorts (Figure 5B).

In order to gain further insight into the differences between upstream *BCL3*-R and CLL, we performed differential methylation analysis between both subgroups of tumors adjusted for trisomy 12, IGHV status, epitype, and

cohort (Figure 5C; *Online Supplementary Figure S7A*). This analysis showed 795 differentially methylated CpG (DMCpG), with 80 hyper- and 715 hypomethylated in *BCL3*-R tumors (q<0.05; log FC=0.25; *Online Supplementary Table S16*). A subset of 21 hypomethylated CpG in *BCL3*-R tumors was modulated during B-cell differentiation, being hypomethylated in germinal center-experienced normal B cells and M-CLL. Unmethylated CpG were enriched in heterochromatin and gene bodies, whereas hypermethylated CpG were enriched in enhancer-promoter regions (*Online Supplementary Figure S7B*). Among the DMCpG, 69 mapped to 37 DEG, with 45 of 64 (70%) hypomethylated CpG lo-

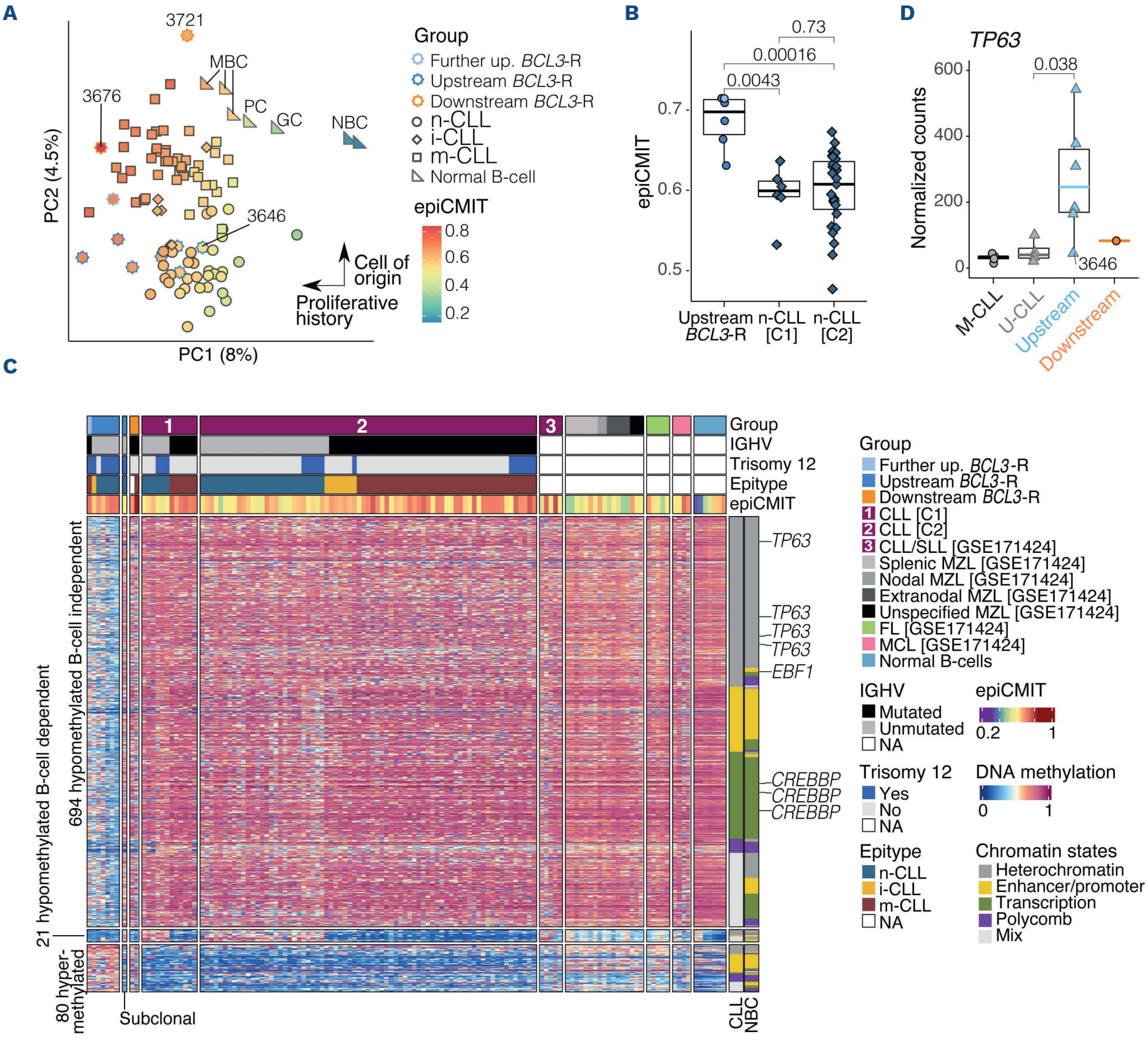

Figure 5. DNA methylation profile of upstream tumors with *BCL3* rearrangement. (A) Principal component analysis (PCA) of DNA methylation data of 10 B-cell neoplasms with *BCL3* rearrangement (*BCL3*-R), 85 chronic lymphocytic leukemia (CLL), and 7 normal B-cells subsets (1st and 2nd components are shown). The shape corresponds to the tumor types while the color represents the proliferative history (epiCMIT score). (B) Comparison of the epiCMIT score between upstream *BCL3*-R tumors and naive-like CLL (n-CLL) from cohorts C1 and C2, respectively. The upstream *BCL3*-R subgroup of tumors does not include the tumor 3646 carrying a subclonal t(14;19). (C) Heatmap of the differentially methylated CpG between 7 upstream *BCL3*-R tumors and 85 CLL. The chromatin state of each CpG is shown on the right. Differentially methylated CpG mapping to differentially expressed CLL genes of interest are labeled. (D) TP63 expression in the upstream *BCL3*-R subgroup compared to CLL. NBC: naive B cell; GC: germinal center B cell; MBC memory B cell; PC: plasma cell; n-CLL: naive-like CLL; i-CLL: intermediate CLL; m-CLL: memory-like CLL; IGHV: variable region of the immunoglobulin heavy chain gene; NA: not available.

cated in the gene body (5'UTR/first exon/body/3'UTR, n=38) or promoter region (TSS1500/TSS200, n=7) of upregulated genes and four of five (80%) hypermethylated CpG mapped to the gene body (n=2) or promoter (n=2) of downregulated genes (Figure 5C; *Online Supplementary Table S16*). These genes include *EBF1*, *CREBBP*, and genes associated with *NOTCH1* pathway (*EPS15L1*, *ZMIZ1*),[27,28] cell proliferation (*BHLHE40*, *TP63*),[29-31] cell motility and migration (*CORO1C*, *GAB1*, *GRAMD1B*, *ITGB2*),[32-36] and poor outcomes in CLL or other lymphoid neoplasms (*IMMP2L*, *OSBPL10*, *TP63*).[31,37,38] Notably, *TP63*, previously shown to be a pro-survival factor in CLL subset #8,[31] was overexpressed in *BCL3*-R cases (Figure 5D). A subsequent transcription factor (TF) binding analysis in the hypomethylated CpG revealed a significant enrichment in the binding sites of B-cell-related TF such as BCL11B, RUNX3, IRF, JUN/FOS, and FOX families (*Online Supplementary Table S17*).

Pathology and clinical characteristics

Given the marked genomic differences between upstream and downstream *BCL3*-R tumors, we reanalyzed their pathological and clinical features separately (Table 1; Figure 6; *Online Supplementary Tables S18, S19*).

Upstream BCL3 rearrangement tumors

Tumor cells in peripheral blood were small medium-sized with condensed non-clumped chromatin and broader pale cytoplasm than expected in typical CLL/SLL. Typical clumped chromatin was observed in only one tumor. Five tumors had cells with indented nuclei and seven tumors had prominent nucleoli (Figure 6A). Lymph node biopsies showed diffuse infiltration by small-to medium-sized cells in all tumors. In two tumors the cells had irregular nuclei and prominent nucleoli. Variable numbers of dispersed large cells were observed in all tumors, but clear proliferation centers were observed in only two. Flow cytometry showed expression of mature B-cell markers with CD5 and CD200 positivity in all tumors, but a typical CLL immunophenotype ($CD19^+$, $CD79b^+$, $CD5^+$, $CD23^+$, $CD43^+$, $CD200^+$ with dim expression of CD20, CD22, and $FMC7^-$) was only found in three of nine tumors (Table 1; *Online Supplementary Table S19*). The other tumors expressed bright B-cell antigens/surface IgG and/or were dim/negative for CD23 and CD43. In the tissue sections, the four tumors studied were LEF1 negative and no or very scant follicular dendritic networks were observed (Figure 6B).

Downstream BCL3-R tumors

Tumor cells in peripheral blood were larger than those in the previous group, and three of four tumors had villi or clasmatosis (Figure 6A). The patient without villous lymphocytes had multiple chromosomal alterations that were not specific to any lymphoid neoplasm. The two lymph nodes examined in these patients had infiltration by atypical small cells that partially preserved the architecture, with open sinusoids and occasional residual germinal centers. Tumor cells expanded the perifollicular areas and colonized germinal centers. One patient showed marked monotypic plasmacytosis. The two spleens showed expansion of the white pulp and partial infiltration of the red pulp by small-to medium-sized lymphoid proliferation with occasional larger cells, consistent with SMZL (Figure 6C). The four tumors expressed strong B-cell markers and were CD5 and CD23 negative. CD200 and CD43 were positive in one of three of the tumors, and two of three expressed IgD. Follicular dendritic cells highlighted the presence of residual germinal centers in all tumors (Figure 6C).

Clinical characteristics

The main clinical difference between the two subgroups was the higher lymphocyte count in the upstream *BCL3*-R subgroup (P=0.01) and splenomegaly in three of the four patients with downstream *BCL3*-R (P=0.07) (Table 1). Two of the latter patients transformed to a large B-cell lymphoma 5 and 11 years after diagnosis. Transformations were not observed in the upstream *BCL3*-R subgroup with a similar median follow-up time as the downstream tumors (6.3 years *vs.* 5.3 years, respectively; P=0.4).

All downstream *BCL3*-R patients required therapy, in contrast to only five of nine patients from the upstream *BCL3*-R subgroup, although no significant differences were found in the median time to first treatment. There were six deaths in the whole cohort, four of which were disease-related, two in the upstream *BCL3*-R subgroup, and two in the downstream *BCL3*-R subgroup, without differences in median survival time. Patients with upstream *BCL3*-R tumors had a similar overall survival as patients with U-CLL and trisomy 12 in our ICGC CLL cohort (*Online Supplementary Figure S8*).

Fluorescence *in situ* hybridization validation of *BCL3* rearrangement breakpoints and expanded cohort

As the current commercially available FISH probes do not distinguish between the 5' and 3' rearrangements of *BCL3*-R identified in this study, we designed a new three-color FISH assay that could identify the new *BCL3* 5' and 3' breakpoints (Figure 7A). We tested the new assay in nine of our 13 tumors and confirmed the breakpoints concordantly with the WGS in all tumors, seven upstream and two downstream (Figure 7B; *Online Supplementary Figure S9A; Online Supplementary Table S1*).

We used the new FISH assay in 17 additional B-cell neoplasms with t(14;19) or *BCL3*-R (*Online Supplementary Table S20, S21*; *Online Supplementary Figure S9B*). We identified an upstream breakpoint in 13 tumors and downstream in four. In line with our previous observations, 11 tumors with upstream breakpoints were diagnosed as

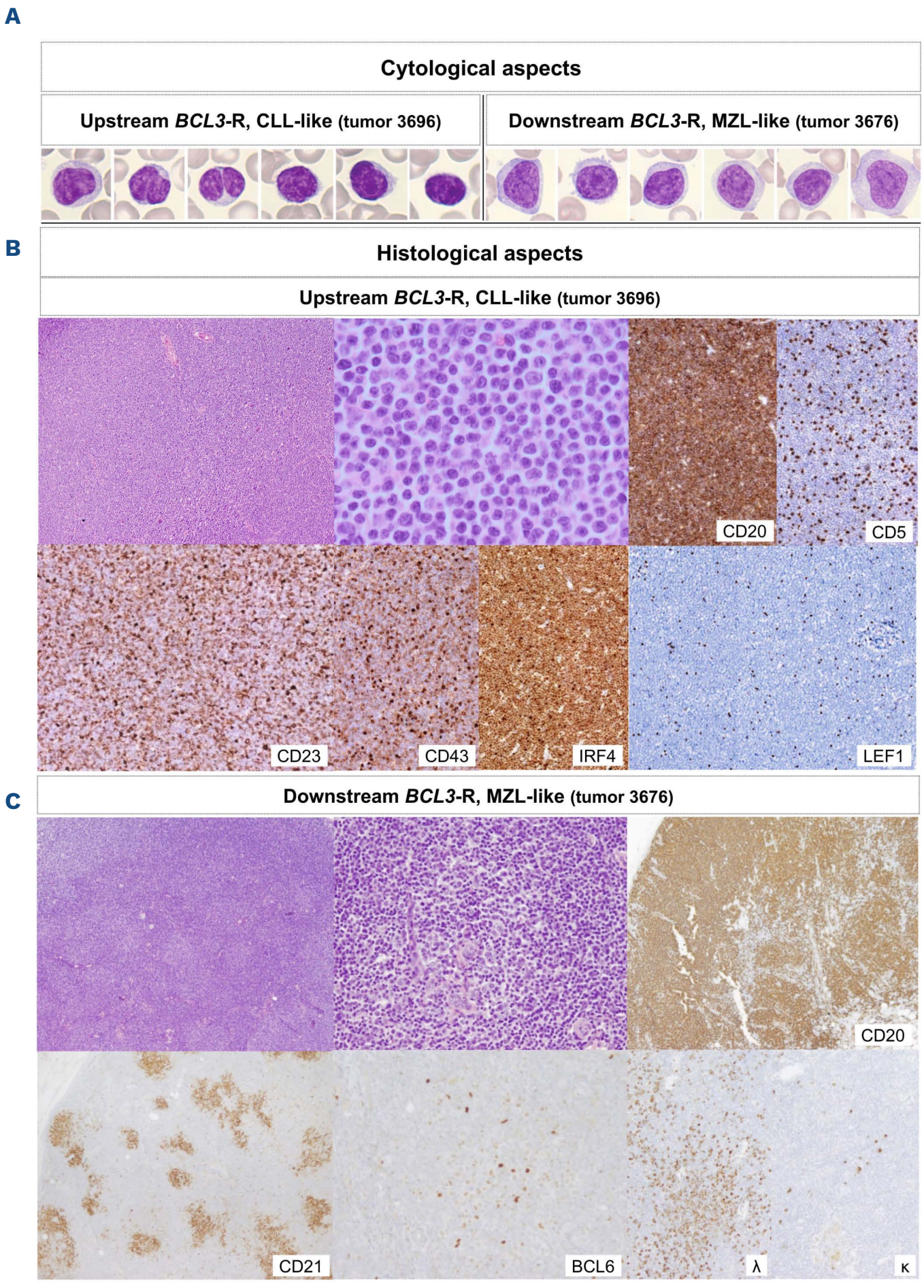

Figure 6. Images of tumors with representative upstream and downstream *BCL3* rearrangement. (A) Cells in peripheral blood smears from representative tumors. Both tumors show features such as nuclear irregularities and lobulation, non-clumped chromatin, central nucleoli, ample cytoplasm, or villi, which are atypical for conventional chronic lymphocytic leukemia (CLL). 1000x oil immersion, light microscope and camera, Leishman stain. (B, C) Histology (hematoxilin & eosin staining) and immunohistochemistry images were obtained from scanned slides (Ventana DP200 scanner, Roche Diagnostics). The upstream *BCL3* rearrangement (*BCL3*-R) tumor had a diffuse growth pattern, resembling chronic lymphocyitc leukemia (CLL), but without proliferation centers (100x). At high power (600x), the cells were small, with scarce cytoplasm, distinct irregular nuclei, and central nucleoli. Larger scattered cells were observed. The immunophenotype is atypical for a CLL tumor ($CD5^-$, $CD23^+$ weak, and $CD43^+$ weak), and the cells are LEF1 negative. CD5 was negative in the lymph nodes by immunohistochemistry but positive in the peripheral blood according to flow cytometry. The downstream *BCL3-R* tumor has a perifollicular growth pattern (100x), leaving residual germinal centers (400x), with a residual follicular dendritic network on CD21 and germinal center cells on BCL6, resembling marginal zone lymphoma. This tumor has a non-specific B-cell phenotype and plasma cell differentiation with κ light-chain restriction. MZL: marginal zone lymphoma.

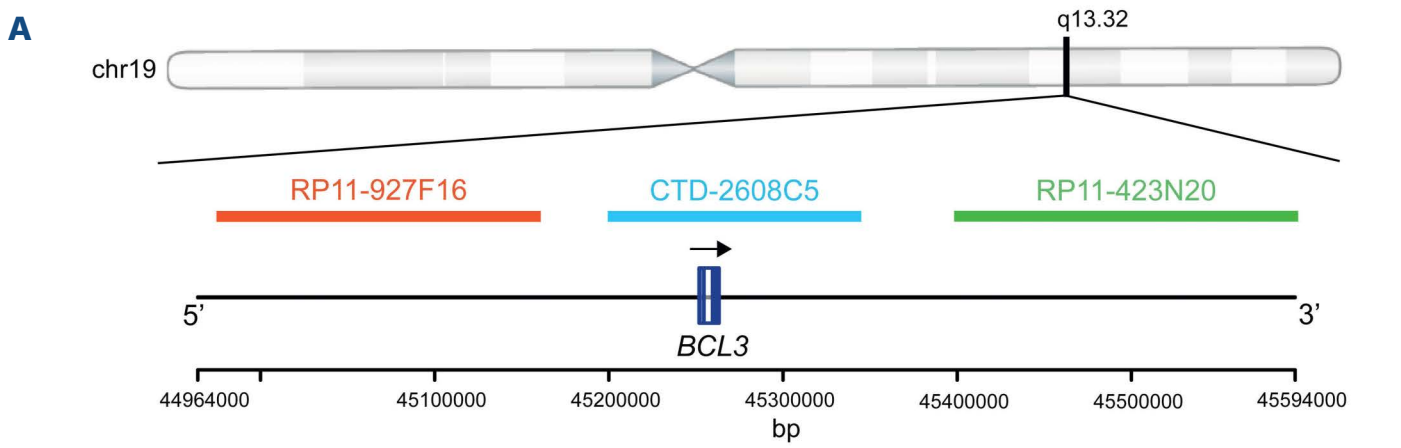

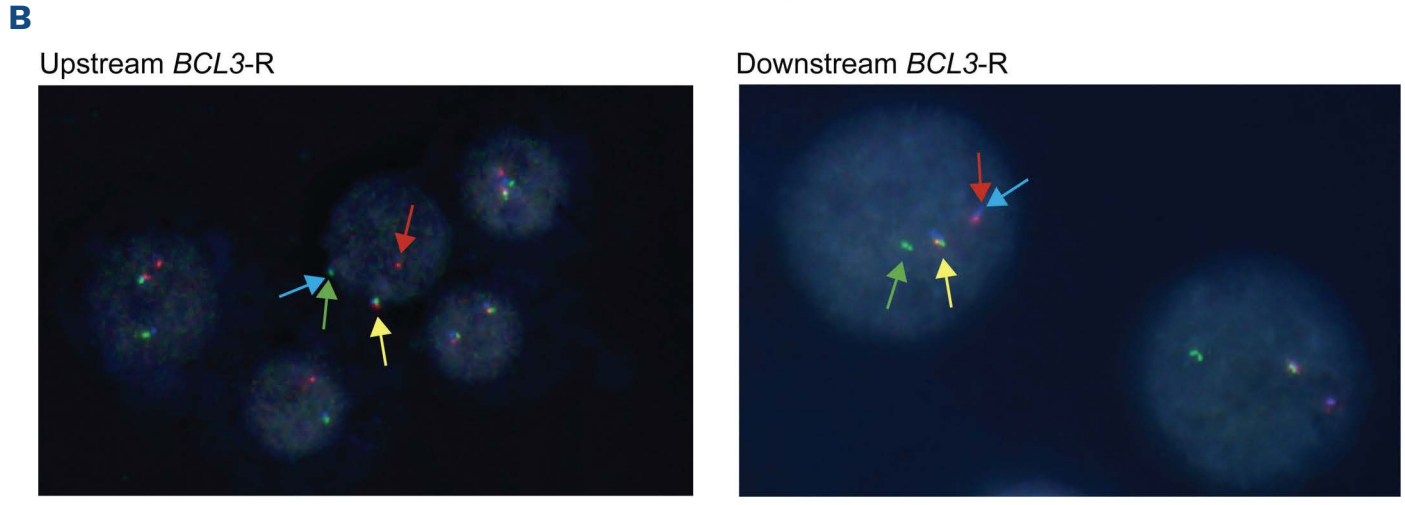

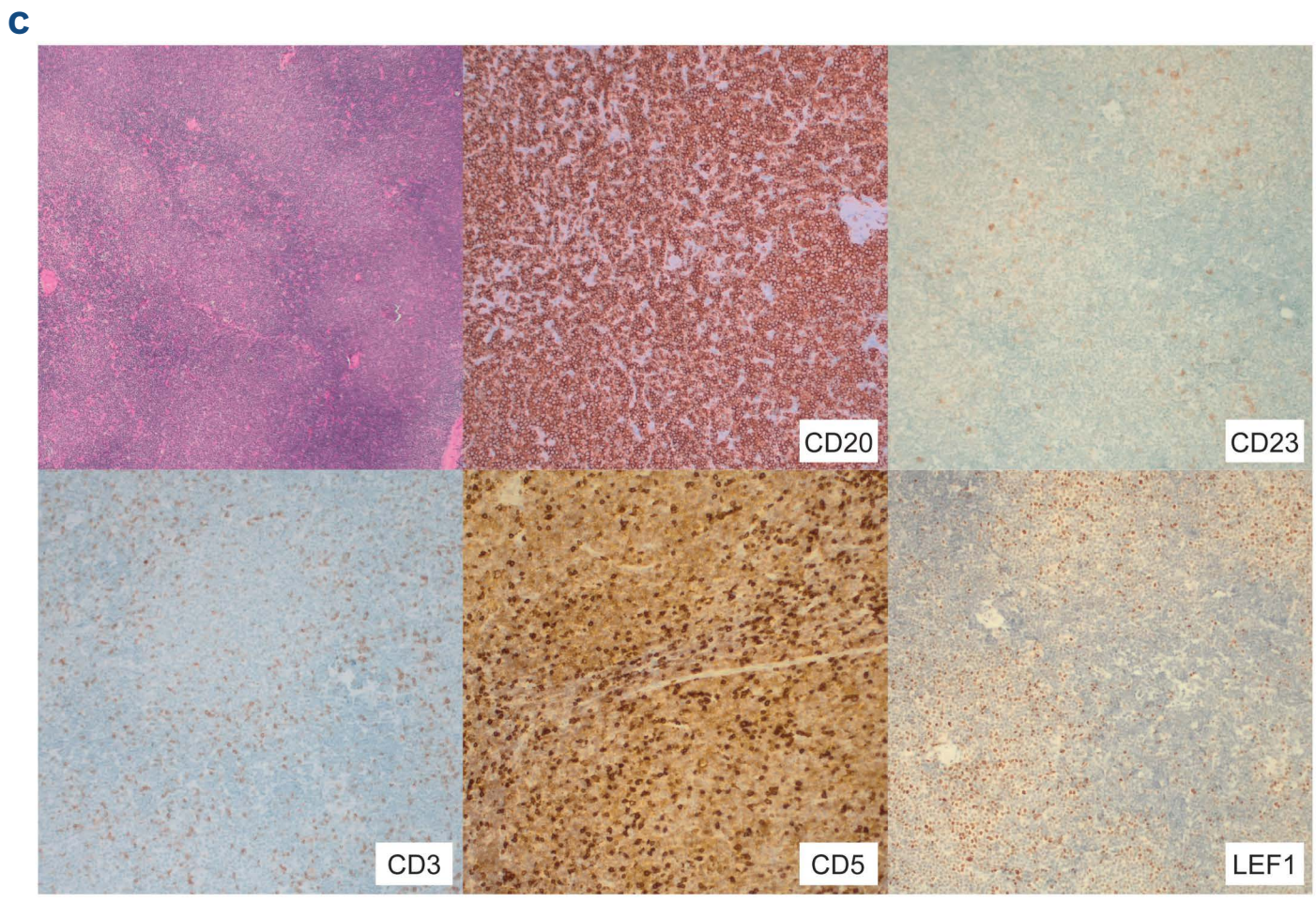

Figure 7. Custom fluorescence *in situ* hybridization assay to map the breakpoints of the *BCL3* rearrangement and images of a representative tumor from the validation cohort. (A) Schematic representation of the custom design of *BCL3* break-apart fluorescence *in situ* hybridization (FISH) probe. *BCL3* gene and *BCL3* FISH probe are annotated based on GRCh37/hg19 assembly. (B) Interphase nucleus of tumor 3783 (left panel) and 3676 (right panel). Tumor 3783 shows a positive signal constellation indicating a break upstream of *BCL3* since the BAC-clone RP11-927F16 is split from CTD2608C5 and RP11-423N20. Tumor 3676 displays a positive signal constellation suggesting a break downstream of *BCL3* with the BAC-clone RP11-423N20 split from CTD2608C5 and RP11-927F16. (C) Histology (hematoxilin & eosin staining) and immunohistochemistry images of tumor 1 from the validation cohort. Low power magnification (50x) of lymph node shows clear proliferation centers. CD20 shows diffuse positivity (100x). CD23 is only partially and faintly expressed in proliferation centers (100x). CD3 highlights few admixed T cells (100x). CD5 shows few admixed T cells (strong staining intensity) and low expression in tumor cells in the lymph node (100x). LEF1 shows expression in T cells and few cells in proliferation centers but mainly negative in tumor cells (100x). *BCL3-R*: *BCL3* rearrangement.

aCLL (n=8) or CLL (n=3) and two as leukemic non-nodal MCL. The aCLL had bright B-cell markers and LEF1 was negative in the six tumors studied. Trisomy 12 was present in eight of eleven and six of seven had U-IGHV. Lymph nodes examined in four cases were consistent with CLL, including prominent proliferation centers in two patients (Figure 7C; *Online Supplementary Figure S10A*). The two MCL were leukemic non-nodal, with *CCND1* rearrangement and overexpression, and SOX11 negative (*Online Supplementary Figure S10B*). Three of the four patients with downstream *BCL3*-R were SMZL, one of them with atypical features previously published,[6] splenomegaly and leukemic disease. Two cases carried del(7)(q32) and one case studied mutations frequent in SMZL (*TNFAIP3*, *NOTCH1*, *KMT2D*) (*Online Supplementary Table S21*).[39]

Discussion

In this study, we characterized the breakpoints of t(14;19) at base-pair resolution in 13 patients with B-cell neoplasms in whom the *BCL3* rearrangement had been detected by FISH. These tumors showed marked molecular, pathological, and clinical differences according to the location of the breakpoint in the 5' or 3' *BCL3* region, suggesting that they correspond to different entities. Specifically, tumors upstream *BCL3*-R showed *BCL3* overexpression, unmutated IGHV, low genomic complexity, trisomy 12, gene mutations and mutational signatures typically observed in CLL. In contrast, tumors with downstream *BCL3*-R did not upregulate *BCL3* and carried M-IGHV, high genomic complexity, and mutations typically observed in MZL. Intriguingly, all the breakpoints in the IGHV were mediated by aberrant CSR, but eight of the nine tumors with the 5' *BCL3* breakpoints had U-IGHV and six of them had 100% identity with the germline, consistent with the fact that CSR occurs before germinal cell commitment and initiation of somatic mutations in the immunoglobulin genes.[40,41]

The pathological features of both subgroups were atypical for CLL or MZL, raising difficulties in their precise taxonomic classification. Upstream *BCL3*-R tumors have characteristics supporting their relationship with CLL including the presence of nodal proliferation centers in some tumors, trisomy 12 in virtually all tumors, and mutations in genes seen in CLL and uncommon in other lymphoid neoplasms. However, the cytological and phenotypic features of most tumors are not completely typical of CLL with bright expression of B-cell antigens and surface Ig, weak or negative CD23 and the expression profile of a subset of genes different from that seen in U-CLL with trisomy 12 such as negative/low expression of *LEF1* and upregulation of *EBF1* among others. In addition, the BCR signaling response was lower than that in U-CLL with trisomy 12. These findings were confirmed in the validation cohort and suggest that lymphoid neoplasms with upstream *BCL3*-R may correspond to a distinct atypical subset of CLL.

Downstream *BCL3*-R tumors had features of MZL with the presence of villous lymphocytes and genetic alterations frequently seen in these tumors (*KLF2*, *NOTCH2*, *TBL1XR1*). However, they also had some atypical characteristics, such as the exclusive leukemic presentation for 5 and 11 years in two patients and large cell transformation in two of them, an event only seen in 10-15% of SMZL cases.[42] Three of four tumors with downstream *BCL3*-R in the validation series were also SMZL, two of them with del(7)(q32).[6] The candidate gene of the downstream *BCL3*-R is unclear. We could only study one of these cases using RNA-seq, which overexpressed *NECTIN2*. This gene, also known as *PVRL2* or CD112, is a member of immunoglobulin-like cell adhesion molecules and a ligand for natural killer cells. Although its potential oncogenic role is unknown, translocations of this gene with IG and T-cell recepetor have been detected in occasional DLBCL and peripheral T-cell lymphomas, respectively.[43,44] Further studies are required to determine whether tumors with downstream *BCL3*-R are a homogeneous group within the marginal zone spectrum.

The biological and clinical differences between tumors with 5' and 3' *BCL3*-R observed in our study may explain the heterogeneity described in the literature. Most of the published tumors resemble our atypical CLL subgroup with an increased frequency of trisomy 12, U-IGHV, and atypical morphology and immunophenotype, although some tumors have also been described as having typical CLL features.[7-9,45] The other subgroup is more heterogeneous with frequent M-IGHV and also MZL characteristics, although with occasional atypical features. Some of the tumors had large B-cell morphology similar to our transformed 3' *BCL3*-R tumors.[6,7,46] The possible prognostic impact of *BCL3*-R in lymphoid neoplasms in the literature is also controversial. Some studies have indicated that CLL or aCLL with *BCL3*-R have an adverse prognosis[8,47-49] but this was not confirmed by others.[50] Our patients with upstream *BCL3*-R had a similar time to the first treatment and overall survival as U-CLL with trisomy 12.

Our new *BCL3*-R FISH assay identified two breakpoints in 11 of 12 (92%) initial tumors studied and in all 17 independent lymphoid neoplasms, 13 with a 5' breakpoint and four with a 3' breakpoint. Interestingly, 11 tumors with upstream *BCL3*-R had pathological and genetic features similar to those of aCLL/CLL with U-IGHV, trisomy 12, and negative LEF1 expression. The tumors with the 3' breakpoint were three SMZL, with some atypical features.[6] These results confirm the value of this new FISH assay in identifying different *BCL3* breakpoints and diseases. The finding of a 5' *BCL3*-R in two nnMCL suggests that, similar

to other translocations in lymphoid neoplasms, *BCL3*-R is not specific to a single entity and needs to be interpreted in the appropriate context.

In conclusion, identification of breakpoints upstream or downstream of *BCL3* revealed two different subgroups of lymphoid neoplasms. Tumors with a 5' breakpoint may correspond to a distinct subset of aCLL/CLL with distinct (epi)genomic, transcriptomic, and clinicopathological features, whereas 3'-rearranged tumors appear to be in the MZL spectrum. We developed a novel FISH assay that recognizes these two *BCL3* breakpoints and is therefore useful in clinical practice to identify the two subgroups of patients.

Disclosures

MJB is currently an employee of Swedish Orphan Biovitrum. FN received honoraria from Janssen, AbbVie, and SOPHiA GENETICS for speaking in educational activities. EC has been a consultant for Takeda, NanoString, AbbVie and Illumina; has received honoraria from Janssen, EUSA Pharma, Takeda and Roche for speaking at educational activities and research funding from AstraZeneca and is an inventor on two patents filed by the National Institutes of Health, National Cancer Institute: "Methods for selecting and treating lymphoma types," licensed to NanoString Technologies, and "Evaluation of mantle cell lymphoma and methods related thereof", not related to this project. FN and EC licensed the use of the protected IgCaller algorithm for Diagnóstica Longwood. The remaining authors have no conflicts of interest to disclose.

Contributions

AC-M analyzed and interpreted the WGS, RNA-seq, and DNA methylation data and wrote the manuscript. FG collected the samples and clinical data, reviewed the histology, and contributed to manuscript preparation. LW reviewed the pathology and contributed to the manuscript preparation. MG performed custom FISH experiments and contributed to the manuscript preparation. RR designed and performed the bioinformatics pipelines for WGS and RNA-seq data analyses and contributed to the manuscript preparation. GF performed the immunohistochemistry experiments and contributed to manuscript preparation. HP performed the calcium flux analyses and contributed to manuscript preparation. MB contributed to the cases, reviewed the pathology, and prepared the manuscript. GC, MD-F, JL, IG, M-JB, JTN, BE, APu, GT, LB, GDC, EB, FC, IR-C, MF-C, EDB, JDN, AP, DV, MR, MA, CS, PB, MP, LY, JXO, ES, TZ, JRC, SHS, JIM-S, DC, EM, SB and DC provided samples and/or data, performed experiments, and interpreted data. FN analyzed and interpreted the data, supervised the bioinformatic analyses, wrote the manuscript, and contributed to the design of the study. EC reviewed and supervised the pathology, analyzed and interpreted the data, wrote the manuscript, and designed the study.

Acknowledgments

The authors thank the Hematopathology Collection registered at the Biobank of Hospital Clínic - Institut d'Investigacions Biomèdiques August Pi i Sunyer (IDIBAPS), the Biobank HUB-ICO-IDIBELL (PT17/0015/0024), integrated in the Spanish Biobank Network and funded by Instituto de Salud Carlos III (PT17/0015/0024), and Xarxa de Bancs de Tumors de Catalunya sponsored by Pla Director d'Oncologia de Catalunya (XBTC), and the Molecular Cytogenetics Platform of IMIM, Hospital del Mar (Barcelona) for providing BAC clones. This work was partially developed at the Center Esther Koplowitz (CEK, Barcelona, Spain).

Funding

This study was supported by the "la Caixa" Foundation (CLLEvolution - LCF/PR/HR17/52150017 [HR17-00221LCF] and CLLSYSTEMS - LCF/PR/HR22/52420015 [HR22-00172] Health Research 2017 and 2022 Programs, to EC), the European Research Council (to EC and JIM-S) under the European Union's Horizon 2020 research and innovation program (810287, BCLLatlas, to EC), Ministry of Science and Innovation (MCIN) /AEI/10.13039/501100011033/ and European Regional Development Fund "Una manera de hacer Europa" (PID2021-123054OB-I00 to EC) and the Generalitat de Catalunya Suport Grups de Recerca AGAUR (2021-SGR-01172 to EC and 2021-SGR-01293 to SB). HP-A is a recipient of a pre-doctoral fellowship from the Spanish Ministry of Science, Innovation and Universities (FPU19/03110). MD-F acknowledges the research support from the AECC Scientific Foundation. FN acknowledges research support from the American Association for Cancer Research (2021 AACR-Amgen Fellowship in Clinical/Translational Cancer Research, 21-40-11-NADE), European Hematology Association (EHA Junior Research Grant 2021, RG-202012-00245), and Lady Tata Memorial Trust (International Award for Research in Leukemia 2021-2022, LADY_TATA_21_3223). EC is an Academia Researcher of the "Institució Catalana de Recerca i Estudis Avançats" (ICREA) of the Generalitat de Catalunya.

Data-sharing statement

Whole genome sequencing, RNA-sequencing, and DNA methylation data are available from the European Genome–phenome Archive (http://www.ebi.ac.uk/ega/) under accession no. EGAS00001007465.

References

1. Michaux L, Mecucci C, Stul M, et al. BCL3 rearrangement and t(14;19)(q32;q13) in lymphoproliferative disorders. Genes Chromosomes Cancer. 1996;15(1):38-47.
2. Palmer S, Chen YH. Bcl-3, a multifaceted modulator of NF-kappaB-mediated gene transcription. Immunol Res. 2008;42(1–3):210–218.
3. Liu H, Zeng L, Yang Y, Guo C, Wang H. Bcl-3: a double-edged sword in immune cells and inflammation. Front Immunol. 2022;13:847699.
4. Zhang X, Paun A, Claudio E, Wang H, Siebenlist U. The tumor promoter and NF-κB modulator Bcl-3 regulates splenic B cell development. J Immunol. 2013;191(12):5984-5992.
5. Ong ST, Hackbarth ML, Degenstein LC, Baunoch DA, Anastasi J, McKeithan TW. Lymphadenopathy, splenomegaly, and altered immunoglobulin production in BCL3 transgenic mice. Oncogene. 1998;16(18):2333-2343.
6. Soma LA, Gollin SM, Remstein ED, et al. Splenic small B-cell lymphoma with IGH/BCL3 translocation. Hum Pathol. 2006;37(2):218-230.
7. Martín-Subero JI, Ibbotson R, Klapper W, et al. A comprehensive genetic and histopathologic analysis identifies two subgroups of B-cell malignancies carrying a t(14;19)(q32;q13) or variant BCL3-translocation. Leukemia. 2007;21(7):1532-1544.
8. Kelly RJ, Wright D, Patil K, et al. t(14;19)(q32;q13) incidence and significance in B-cell lymphoproliferative disorders. Br J Haematol. 2008;141(4):561-563.
9. Huh YO, Schweighofer CD, Ketterling RP, et al. Chronic lymphocytic leukemia with t(14;19)(q32;q13) is characterized by atypical morphologic and immunophenotypic features and distinctive genetic features. Am J Clin Pathol. 2011;135(5):686-696.
10. Li H, Durbin R. Fast and accurate short read alignment with Burrows-Wheeler transform. Bioinformatics. 2009;25(14):1754-1760.
11. Nadeu F, Mas-de-les-Valls R, Navarro A, et al. IgCaller for reconstructing immunoglobulin gene rearrangements and oncogenic translocations from whole-genome sequencing in lymphoid neoplasms. Nat Commun. 2020;11(1):3390.
12. Brochet X, Lefranc M-P, Giudicelli V. IMGT/V-QUEST: the highly customized and integrated system for IG and TR standardized V-J and V-D-J sequence analysis. Nucleic Acids Res. 2008;36(Web Server issue):W503-508.
13. Nadeu F, Royo R, Massoni-Badosa R, et al. Detection of early seeding of Richter transformation in chronic lymphocytic leukemia. Nat Med. 2022;28(8):1662-1671.
14. Love MI, Huber W, Anders S. Moderated estimation of fold change and dispersion for RNA-seq data with DESeq2. Genome Biol. 2014;15(12):550.
15. Puente XS, Beà S, Valdés-Mas R, et al. Non-coding recurrent mutations in chronic lymphocytic leukaemia. Nature. 2015;526(7574):519-524.
16. Lu J, Cannizzaro E, Meier-Abt F, et al. Multi-omics reveals clinically relevant proliferative drive associated with mTOR-MYC-OXPHOS activity in chronic lymphocytic leukemia. Nat Cancer. 2021;2(8):853-864.
17. Ritchie ME, Phipson B, Wu D, et al. limma powers differential expression analyses for RNA-sequencing and microarray studies. Nucleic Acids Res. 2015;43(7):e47.
18. Aryee MJ, Jaffe AE, Corrada-Bravo H, et al. Minfi: a flexible and comprehensive Bioconductor package for the analysis of Infinium DNA methylation microarrays. Bioinformatics. 2014;30(10):1363-1369.
19. Bailey TL, Johnson J, Grant CE, Noble WS. The MEME suite. Nucleic Acids Res. 2015;43(W1):W39-W49.
20. Castro-Mondragon JA, Riudavets-Puig R, Rauluseviciute I, et al. JASPAR 2022: the 9th release of the open-access database of transcription factor binding profiles. Nucleic Acids Res. 2022;50(D1):D165-D173.
21. Ventura RA, Martin-Subero JI, Jones M, et al. FISH analysis for the detection of lymphoma-associated chromosomal abnormalities in routine paraffin-embedded tissue. J Mol Diagn. 2006;8(2):141-151.
22. Navarro A, Clot G, Martínez-Trillos A, et al. Improved classification of leukemic B-cell lymphoproliferative disorders using a transcriptional and genetic classifier. Haematologica. 2017;102(9):e360-e363.
23. Seifert M, Sellmann L, Bloehdorn J, et al. Cellular origin and pathophysiology of chronic lymphocytic leukemia. J Exp Med. 2012;209(12):2183-2198.
24. Gutierrez A, Tschumper RC, Wu X, et al. LEF-1 is a prosurvival factor in chronic lymphocytic leukemia and is expressed in the preleukemic state of monoclonal B-cell lymphocytosis. Blood. 2010;116(16):2975-2983.
25. Kulis M, Heath S, Bibikova M, et al. Epigenomic analysis detects widespread gene-body DNA hypomethylation in chronic lymphocytic leukemia. Nat Genet. 2012;44(11):1236-1242.
26. Duran-Ferrer M, Clot G, Nadeu F, et al. The proliferative history shapes the DNA methylome of B-cell tumors and predicts clinical outcome. Nat Cancer 2020;1(11):1066–1081.
27. Griffen TL, Dammer EB, Dill CD, et al. Multivariate transcriptome analysis identifies networks and key drivers of chronic lymphocytic leukemia relapse risk and patient survival. BMC Med Genomics. 2021;14(1):171.
28. Pinnell N, Yan R, Cho HJ, et al. The PIAS-like coactivator Zmiz1 is a direct and selective cofactor of Notch1 in T cell development and leukemia. Immunity. 2015;43(5):870-883.
29. Cook ME, Jarjour NN, Lin C-C, Edelson BT. Transcription factor Bhlhe40 in immunity and autoimmunity. Trends Immunol. 2020;41(11):1023-1036.
30. Rauschmeier R, Reinhardt A, Gustafsson C, et al. Bhlhe40 function in activated B and TFH cells restrains the GC reaction and prevents lymphomagenesis. J Exp Med. 2022;219(2):e20211406.
31. Papakonstantinou N, Ntoufa S, Tsagiopoulou M, et al. Integrated epigenomic and transcriptomic analysis reveals TP63 as a novel player in clinically aggressive chronic lymphocytic leukemia. Int J Cancer. 2019;144(11):2695-2706.
32. Roadcap DW, Clemen CS, Bear JE. The role of mammalian coronins in development and disease. Subcell Biochem. 2008;48:124-135.
33. Seda V, Vojackova E, Ondrisova L, et al. FoxO1-GAB1 axis regulates homing capacity and tonic AKT activity in chronic lymphocytic leukemia. Blood. 2021;138(9):758-772.
34. Khanna P, Lee JS, Sereemaspun A, Lee H, Baeg GH. GRAMD1B regulates cell migration in breast cancer cells through JAK/STAT and Akt signaling. Sci Rep. 2018;8(1):9511.
35. Hutterer E, Asslaber D, Caldana C, et al. CD18 (ITGB2) expression in chronic lymphocytic leukaemia is regulated by DNA methylation-dependent and -independent mechanisms. Br J Haematol. 2015;169(2):286-289.
36. Goldin LR, McMaster ML, Rotunno M, et al. Whole exome sequencing in families with CLL detects a variant in Integrin β 2

associated with disease susceptibility. Blood. 2016;128(18):2261-2263.
37. Dobashi A, Togashi Y, Tanaka N, et al. TP53 and OSBPL10 alterations in diffuse large B-cell lymphoma: prognostic markers identified via exome analysis of cases with extreme prognosis. Oncotarget. 2018;9(28):19555-19568.
38. Schweighofer CD, Coombes KR, Majewski T, et al. Genomic variation by whole-genome SNP mapping arrays predicts time-to-event outcome in patients with chronic lymphocytic leukemia: a comparison of CLL and HapMap genotypes. J Mol Diagn. 2013;15(2):196-209.
39. Grau M, López C, Navarro A, et al. Unraveling the genetics of transformed splenic marginal zone lymphoma. Blood Adv. 2023;7(14):3695-3709.
40. Oppezzo P, Vuillier F, Vasconcelos Y, et al. Chronic lymphocytic leukemia B cells expressing AID display dissociation between class switch recombination and somatic hypermutation. Blood. 2003;101(10):4029-4032.
41. Roco JA, Mesin L, Binder SC, et al. Class-switch recombination occurs infrequently in germinal centers. Immunity. 2019;51(2):337-350.
42. Bastidas-Mora G, Beà S, Navarro A, et al. Clinico-biological features and outcome of patients with splenic marginal zone lymphoma with histological transformation. Br J Haematol. 2022;196(1):146-155.
43. Otto C, Scholtysik R, Schmitz R, et al. Novel IGH and MYC translocation partners in diffuse large B-cell lymphomas. Genes Chromosomes Cancer. 2016;55(12):932-943.
44. Almire C, Bertrand P, Ruminy P, et al. PVRL2 is translocated to the TRA@ locus in t(14;19)(q11;q13)-positive peripheral T-cell lymphomas. Genes Chromosomes Cancer. 2007;46(11):1011-1018.
45. Chapiro E, Radford-Weiss I, Bastard C, et al. The most frequent t(14;19)(q32;q13)-positive B-cell malignancy corresponds to an aggressive subgroup of atypical chronic lymphocytic leukemia. Leukemia. 2008;22(11):2123-2127.
46. Salido M, Baró C, Oscier D, et al. Cytogenetic aberrations and their prognostic value in a series of 330 splenic marginal zone B-cell lymphomas: a multicenter study of the Splenic B-Cell Lymphoma Group. Blood. 2010;116(9):1479-1488.
47. Busschots AM, Mecucci C, Stul M, et al. Translocation (14;19)(q32;q13.1) in a young patient who developed a large cell lymphoma after an initial diagnosis of CLL. Leuk Lymphoma. 1991;5(4):281-286.
48. Michaux L, Dierlamm J, Wlodarska I, Bours V, Van Den Berghe H, Hagemeijer A. t(14;19)/BCL3 rearrangements in lymphoproliferative disorders: a review of 23 cases. Cancer Genet Cytogenet. 1997;94(1):36-43.
49. Fang H, Reichard KK, Rabe KG, et al. IGH translocations in chronic lymphocytic leukemia: Clinicopathologic features and clinical outcomes. Am J Hematol. 2019;94(3):338-345.
50. Rossi D, Deambrogi C, Monti S, et al. BCL3 translocation in CLL with typical phenotype: assessment of frequency, association with cytogenetic subgroups, and prognostic significance. Br J Haematol. 2010;150(6):702-704.